Electron solvation dynamics in $I^-(NH_3)_n$ clusters

Christian Frischkorn,[ab] Martin T. Zanni,[ab] Alison V. Davis[ab] and Daniel M. Neumark*[ab]

[a] *Department of Chemistry, University of California, Berkeley, CA 94720, USA and*
[b] *Chemical Sciences Division, Lawrence Berkeley National Laboratory, Berkeley, CA, 94720, USA*

Received 15th December 1999
Published on the Web 10th April 2000

Femtosecond photoelectron spectroscopy (FPES) is used to monitor the dynamics associated with the excitation of the charge-transfer-to-solvent (CTTS) precursor states in $I^-(NH_3)_{n=4-15}$ clusters. The FPE spectra imply that the weakly bound excess electron in the excited state undergoes partial solvation *via* solvent rearrangement on a time scale of 0.5–2 ps, and this partially solvated state decays by electron emission on a 10–50 ps time scale. Both the extent of solvation and the lifetimes increase gradually with cluster size, in contrast to the more abrupt size-dependent effects previously observed in $I^-(H_2O)_n$ clusters.

Introduction

For almost a century, the solvated electron has attracted much attention for its importance in many areas of chemistry including radiation chemistry, electron transfer, and charge-induced reactivity. In 1864, unaware of its origin, Weyl[1] discovered a brilliant blue color in experiments dissolving metals in liquid ammonia. This observation was not attributed to solvated electrons until the beginning of this century,[2] resulting in many studies of stable solvated electrons in bulk ammonia.[3,4] Even more interest was generated by the discovery in 1962 of hydrated electrons in bulk water by Hart and Boag.[5] Further research on solvated electrons[6–8] in the bulk has included other polar solvents such as alcohols.[9,10] More recently, time-resolved measurements with femtosecond resolution have been performed in order to address the photoinitiated dynamics associated with electron solvation, with most of this effort focused on hydration.[11–15]

The experiments on solvated electrons in solution raise an interesting issue from the perspective of cluster physics and chemistry: how are the properties of a solvated electron manifested in a system of finite size? Unlike bulk ammonia, an individual NH_3 molecule does not bind an excess electron. However, measurements done by Haberland *et al.*[16] and Lee *et al.*[17] showed that $(NH_3)_n^-$ cluster anions with $n \geqslant 35$ are stable. Lee *et al.*[17] also determined size-dependent vertical detachment energies for $(NH_3)_n^-$ clusters using photoelectron spectroscopy, finding an apparent extrapolation to the ionization potential of liquid ammonia. Theoretical studies by Barnett *et al.*[18] and Marchi *et al.*[19] have been carried out using quantum path-integral molecular dynamics and Monte Carlo methods, respectively. Both calculations predict that the excess electron binds to the surface of the cluster for small clusters, and that "interior" states in which the electron is surrounded by solvent molecules require larger clusters. The calculation by Barnett *et al.*[18] predicts that the $n = 32$ cluster is the smallest that supports an interior state. The agreement of this value

with the onset of stability of negatively charged $(NH_3)_n^-$ clusters at $n = 35$ supports the assertion made in the experimental papers that these species are the cluster counterparts of bulk ammoniated (solvated) electrons.

Since solvated electrons in ammonia can be created by the spontaneous ionization of an alkali metal in bulk ammonia, finite $M(NH_3)_n$ clusters (where M is an alkali atom) are also of considerable interest as model finite systems for cluster solvation. Hertel and co-workers,[20–22] Fuke and co-workers,[23–25] have performed a series of measurements on the ionization potentials and absorption spectroscopy of neutral $M(NH_3)_n$ clusters, while Fuke and co-workers[24,25] have measured photoelectron spectra of size-selected $M^-(NH_3)_n$ cluster anions. These measurements along with electronic structure calculations[26] indicate that the first solvation shell of the neutral clusters consists of four ammonia molecules, and clusters as small as $M(NH_3)_4$ show evidence for delocalization of the outermost electron on the alkali atom into the surrounding solvent molecules.

In this paper, we undertake a complementary approach to electron solvation in ammonia through spectroscopic and dynamical studies of $I^-(NH_3)_n$ clusters. This work is motivated by previous studies of $I^-(H_2O)_n$ clusters, in particular the frequency-domain electronic spectroscopy performed by Serxner *et al.*[27] and femtosecond photoelectron spectroscopy (FPES) experiments carried out in our laboratory.[28] In the electronic ground state of $I^-(H_2O)_n$ clusters, the excess electron is localized on the halogen. However, while isolated I^- has no excited electronic states in the vicinity of the electron detachment threshold, the clusters exhibit a broad absorption band that blue-shifts as the number of water molecules is increased, apparently converging to the lower of the two charge-transfer-to-solvent (CTTS) bands seen in aqueous I^- solutions.[29,30] In solution, excitation of the CTTS bands ejects an electron from the halide into the solvent, ultimately yielding a hydrated electron.[31] The dynamics of this process have attracted both experimental[32,33] and theoretical interest.[34,35] Hence, experiments on $I^-(H_2O)_n$ or $I^-(NH_3)_n$ clusters offer another means of probing electron solvation in systems of finite extent.

In the frequency-domain study by Serxner *et al.*[27] it was pointed out that the solvent network in the ground state of $I^-(H_2O)_n$ clusters has a dipole moment large enough to bind an electron (4.4 D for $n = 4$, based on the calculated structure by Combariza *et al.*[36]). The excited electronic state was attributed to a dipole-bound state (DBS) in which the excess electron is bound by the high dipole moment of the solvent network. Our FPE spectra of $I^-(H_2O)_4$ indicated that this excited state decays with a 2.8 ps time constant.[28] Very different dynamics were observed for clusters with $n > 4$. The FPE spectra suggest that in these larger clusters, the electron is initially photoexcited to a DBS. However, after several hundred femtoseconds, the spectra abruptly shift to higher electron binding energy, indicating the excess electron is stabilized by rearrangement of the solvent molecules. This "partially solvated" state decays on a time scale varying from tens to hundreds of ps, depending on the number of water molecules. Hence, five water molecules appear to be the minimum required to observe electron solvation in the excited state of $I^-(H_2O)_n$ clusters.

Here, we present FPE spectra of $I^-(NH_3)_n$ clusters in order to explore the solvent-dependence of electron solvation dynamics in this class of clusters. In the FPES experiment, an ultrafast pump pulse excites an electron initially localized on the iodide ion. This excess electron is then detached with a second, time-delayed ultrafast probe pulse, and recording the photoelectron spectra as a function of the delay time provides the means to trace the temporal evolution of the photoexcited state. Our results show significantly different electron solvation dynamics in $I^-(NH_3)_n$ clusters compared to $I^-(H_2O)_n$. The onset of electron solvation dynamics is more gradual in $I^-(NH_3)_n$ clusters, and there is no obvious critical size for electron solvation. There is also no evidence for an initially excited DBS. Finally, the lifetime of the partially solvated state is considerably shorter than in comparably sized $I^-(H_2O)_n$ clusters.

Experimental

The FPES apparatus has been described in detail elsewhere.[37,38] Only a brief summary will be given here, highlighting the specific features necessary to accomplish the experiments presented in this paper. To generate cold iodide–ammonia clusters, a premixture of 0.9% NH_3 in Ar passes over a reservoir of CH_3I at a stagnation pressure of 1.5 bar and is then expanded supersonically into the vacuum chamber through a pulsed valve operating at a repetition rate of 500 Hz. Just downstream of the nozzle, the resulting free jet is crossed by a 1 keV electron beam producing ions

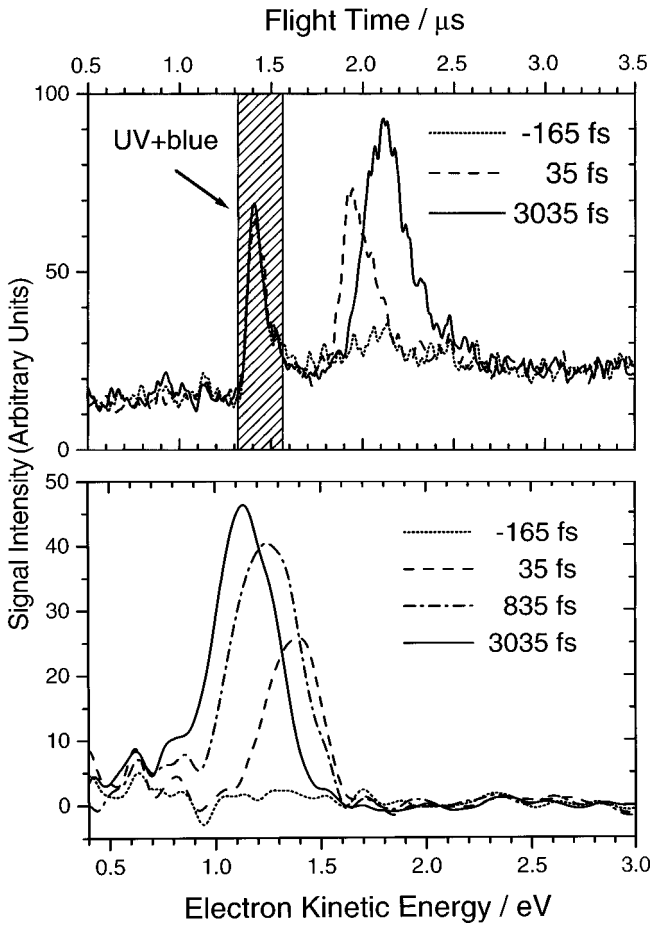

Fig. 1 Experimental FPE spectra of $I^-(NH_3)_{15}$ at various delay times ranging from −165 fs to 3035 fs. The upper panel shows raw electron time-of-flight data and illustrates the normalization scheme used in a 3-color setup; the 2-photon signal originating from the UV and blue, which is kept at a fixed delay, serves as a reference peak while the relative timing between UV and red is varied to monitor the time evolution of the excited state. The lower panel displays several normalized photoelectron spectra, which show a clear shift to lower eKE with increasing delay time.

that undergo clustering as the expansion proceeds. The free jet is skimmed, and the anions are injected into a Wiley–McLaren time-of-flight mass spectrometer[39] by applying pulsed extraction and acceleration fields perpendicular to the expansion axis. After passing through several differentially pumped regions, the mass-selected anions interact with the ultrafast excitation and detachment laser pulses at the focus of a photoelectron time-of-flight analyzer with a "magnetic bottle"[40] providing a high collection efficiency (>50%) for the photoelectrons. The electron arrival time distribution is recorded after each laser shot with a multi-channel scalar (MCS, Stanford Research Systems SR430), which is read out by a computer for data storage and further processing of the PE spectra.

At a repetition rate that matches that of the pulsed valve, a Ti : sapphire oscillator-regenerative amplifier laser system (Clark MXR) generates pulses with 80 fs full width half maximum (FWHM, $sech^2$) in time duration and 1 mJ in pulse energy. The center wavelength of the pulses is generally 790 nm but this is tuned somewhat as needed. The major portion (70%) of the fundamental light is either used to pump an optical parametric amplifier (TOPAS, Light Conversion) optimized at 790 nm pump wavelength or frequency tripled in a BBO-crystal based tripling unit, depending on the

cluster size. To excite $I^-(NH_3)_{n=4-6}$ clusters, the signal output of the TOPAS is frequency-quadrupled (applying second harmonic generation (SHG) twice) which provides pulses of 6–10 μJ and 150 fs FHWM ($sech^2$) in the wavelength range of 370–320 nm (3.35–3.87 eV). For the larger clusters, excitation to the CTTS states is achieved using frequency-tripled pulses in the UV (20 μJ and 110 fs FHWM ($sech^2$)) at 273 nm (4.54 eV) and 263 nm (4.71 eV) for $n = 8$ and $n \geqslant 9$, respectively. For all clusters, the remainder of the fundamental is time-delayed with respect to the UV light *via* a computer-controlled translation stage and serves as the probe. Two-color above-threshold detachment (ATD)[41] of I^- is used to characterize the pump and probe pulses and to determine the zero of time inside the vacuum chamber.

In order to compare FPE spectra at different delay times, various data collection and normalization schemes are applied. For the smaller clusters $I^-(NH_3)_{n=4-6}$, normalization is accomplished by alternating between 10 s scans at the desired delay and 3 s scans at a fixed, positive delay time (1 ps) for reference. Each spectrum is normalized according the integrated count rate of its associated reference scan. The data acquisition time ratio of 3 : 1 is chosen to maximize signal acquisition time while accounting for possible signal fluctuations on a time scale of a few seconds affecting both scans at the variable and the fixed delay. In addition, to compensate longer-time signal drifts, it is preferable to accumulate several series of shorter scans (6–10 s, 3000–5000 laser shots per scan) at each delay than to record longer scans with up to 10 000 laser shots (20 s) per scan. Depending on the signal-to-noise ratio, a total number of 20 000 to 40 000 laser shots per delay time is collected.

In the laser setup for the larger clusters ($8 \leqslant n \leqslant 15$), the residual frequency-doubled light from the tripling unit is used to create a two-photon reference signal as follows. An optical chopper (New Focus 3501) alternately blocks the probe fundamental (red) and the frequency-doubled light (blue), which is kept at a fixed, positive delay with respect to the pump (UV). The UV-blue signal created at every other laser shot serves as a reference, so normalization to this signal accounts for both the short-time and the longer-time signal fluctuations on a scale of a couple of seconds and several tens of minutes, respectively. In addition, for the $I^-(NH_3)_{n=8-10}$ PE spectra, shot-to-shot background subtraction is performed on the MCS to account for UV-only detachment signal of neighboring ion masses which partially overlap the desired two-photon signal. As an example of the normalization applied in the three-color version of the experiment, the upper panel of Fig. 1 displays raw electron time-of-flight spectra for $I^-(NH_3)_{15}$ at three different delay times. The time-dependent UV-red signal is scaled according its individual UV-blue reference peak, and the resulting normalized FPE spectra are shown in the bottom panel of Fig. 1.

Results

Since the cluster CTTS states are expected to lie near the detachment threshold, one-photon photoelectron spectra of $I^-(NH_3)_n$ clusters were measured. These spectra are shown in Fig. 2 as a function of the electron kinetic energy (eKE) for the bare I^- anion and the clusters $I^-(NH_3)_{n=1-8}$ at a photodetachment wavelength of 263 nm (4.71 eV). Up to $n = 2$, this excitation energy is sufficient to detach the anion to both final spin–orbit states ($^2P_{3/2,\,1/2}$) of the neutral. The energy resolution of the PE spectra is only moderate (*ca.* 250 meV for 1 eV eKE at the I^- mass). The peaks of the smaller clusters ($n \leqslant 2$) consist of a double structure due to superposition of the velocities of the parent ion and the ejected electron. The vertical detachment energy VDE(n) for $I^-(NH_3)_n$ is obtained from the electron kinetic energy of the peak maximum (eKE_{max}) using

$$VDE(n) = h\nu - eKE_{max} \quad (1)$$

and represents the energy needed to remove an electron with no change in geometry.

The difference between VDE(n) and VDE($n = 0$) represents the energy E_{stab}, by which a specific cluster size with n solvent molecules is stabilized with respect to bare I^-. For the lower spin–orbit state of the iodide core ($J = 3/2$), Fig. 3 shows both the vertical detachment energy (left axis) and E_{stab} (right axis) as a function of the number of NH_3 molecules. In the measured size range $0 \leqslant n \leqslant 8$, no leveling-off of E_{stab} is found which might otherwise indicate a possible closure of a solvation shell.

Using the measured VDEs as a starting point, optimal pump wavelengths for the CTTS states with $n \leqslant 8$ were found empirically by maximizing the two-color photoelectron signal. For $n = 4$, 5,

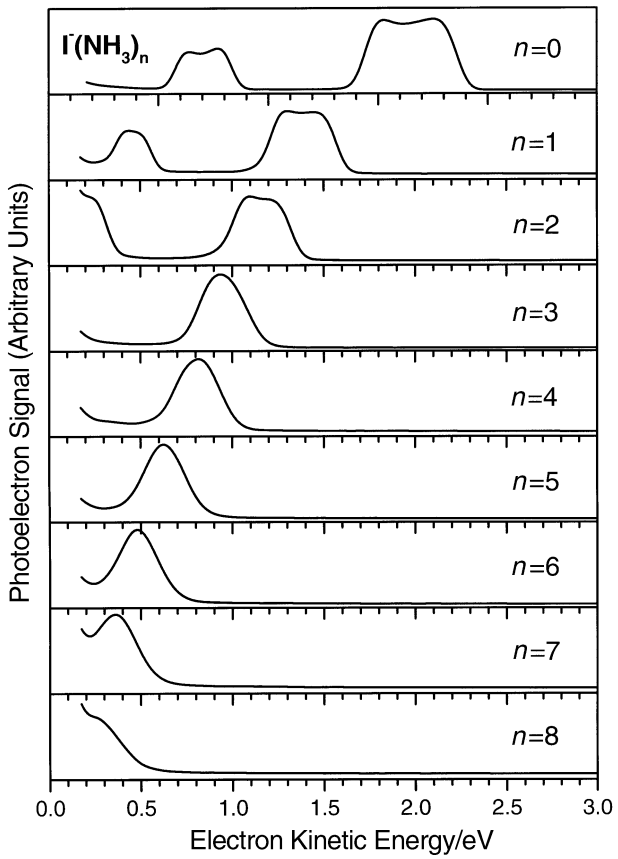

Fig. 2 1-color photoelectron spectra of $I^-(NH_3)_{n=0-8}$ clusters at a photodetachment wavelength of 263 nm (4.71 eV).

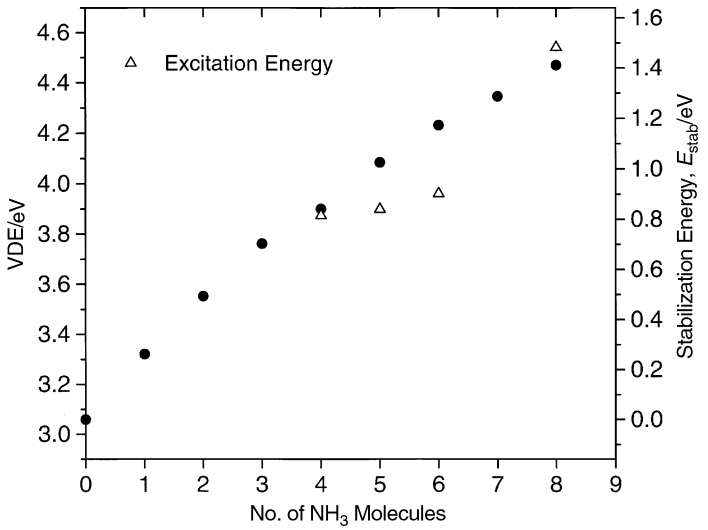

Fig. 3 Vertical detachment energy VDE of $I^-(NH_3)_{n=0-8}$ (left axis) and stabilization energy E_{stab} = VDE(n) − VDE(0) for the clusters with respect to bare I^- (right axis) as a function of the number of solvent molecules. The open triangle (△) mark the excitation energies of the pump pulse used in the FPES experiments.

6 and 8, the pump wavelengths were 320 nm, 318 nm, 313 nm and 273 nm, respectively (also shown in Fig. 3). No obvious pattern can be seen for the relative position of the optimal excitation energy with respect to the VDE, but we point out that our goal was to maximize FPES signal rather than characterize the cluster CTTS state. For the larger clusters studied ($n = 9$, 10, 12, 13 and 15), frequency-tripled UV light at 263 nm provided sufficient overlap with the CTTS transition.

Fig. 4 shows FPE spectra of $I^-(NH_3)_{n=4-6,\,8,\,10,\,15}$ as two-dimensional (2D) contour plots. The PE intensity is coded in different gray-scales (dark : high intensity, light : low intensity) as a function of eKE (left y-axis) and electron binding energy (eBE $\equiv h\nu_{probe} - eKE$, right y-axis) *vs.* pump–probe delay. Each slice parallel to the y-axis represents a complete PE spectrum at a specific delay time Δt, several of which are shown for the $n = 15$ cluster in the lower panel of Fig. 1. Displaying the data in contour plots allows one to conveniently identify any change of the shape or position of the spectra as time evolves.

At any given delay time, the photoelectron spectrum consists of a single peak, and by tracking the peak maximum we obtain time-dependent VDEs that concisely represent the dynamics in the evolving excited state. Fig. 5 (upper panel) shows a plot of the VDE *vs.* time for several $I^-(NH_3)_n$ clusters during the first 3 ps (we refer to this interval as "short-time"). The VDE at the earliest observation times increases with cluster size, from 0.1 eV for $n = 4$ to 0.2 eV for $n = 15$. In all cases, the VDE rises over the time interval in Fig. 5. For the smallest cluster studied, $I^-(NH_3)_4$, a small but non-zero increase in the VDE of 70 meV is seen; this shift in VDE builds up steadily with n until reaching a value of $\sim$220 meV for $n = 8$, above which no further increase is seen. We also obtained time constants τ_{shift} associated with this energy shift from a single exponential fit to the data of Fig. 5. These start at 780 fs for $n = 4$, decrease with increasing cluster size reaching a

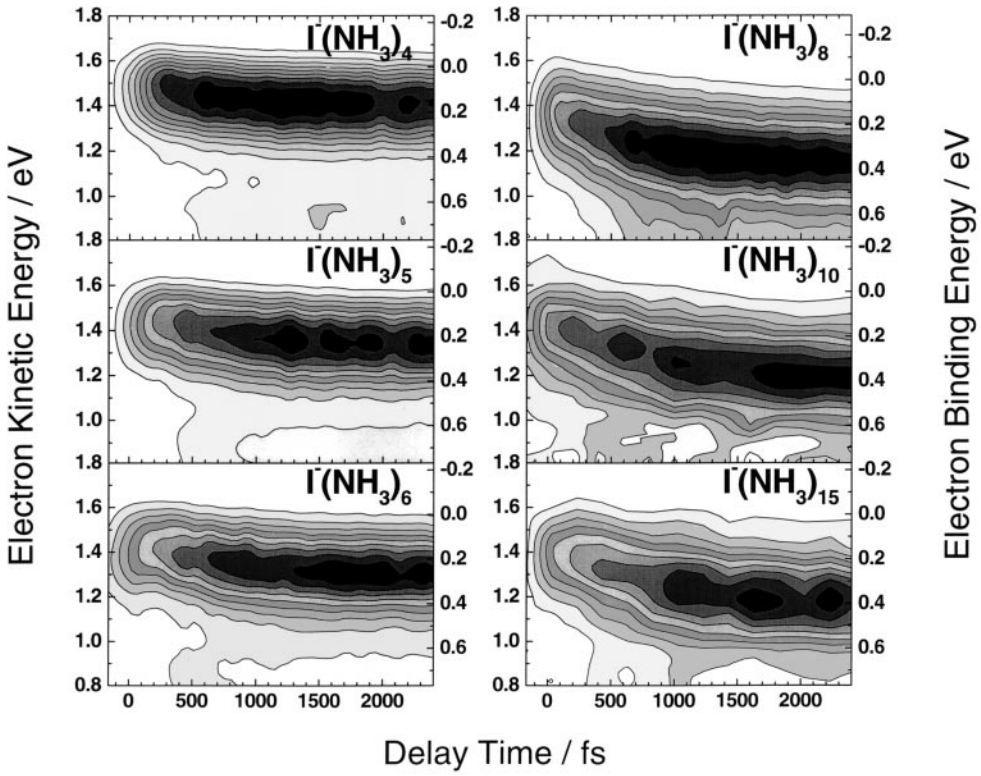

Fig. 4 FPE spectra of $I^-(NH_3)_n$ ($n = 4$–6, 8, 10 and 15) as two-dimensional contour plots of eKE (left y-axis) and eBE (right y-axis), respectively, *vs.* pump–probe delay. Note that the probe wavelength for $n = 8$ differs from that used for all other cluster sizes.

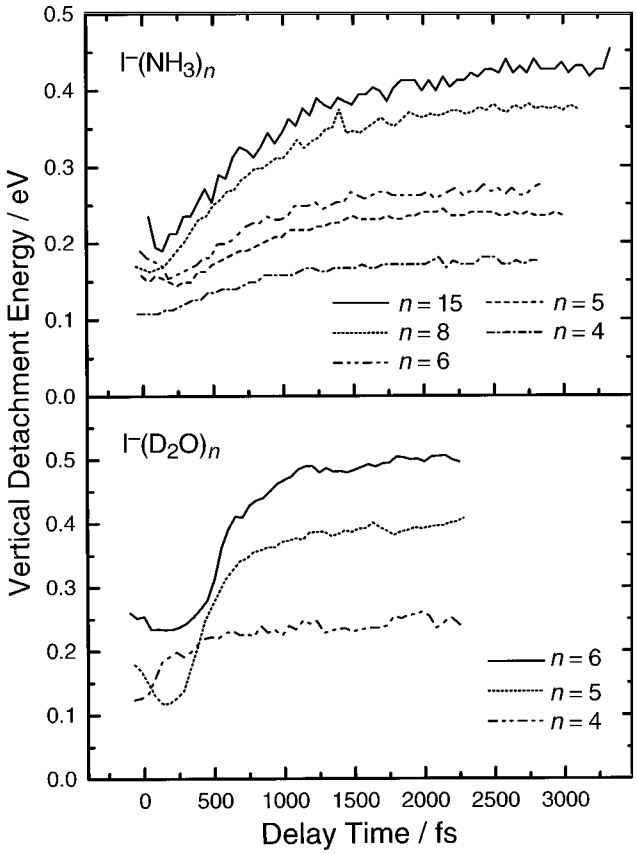

Fig. 5 Time evolution of the vertical detachment energy VDE for $I^-(NH_3)_n$ clusters, $n = 4$–6, 8 and 15 (upper panel). For comparison, results for $I^-(D_2O)_n$ clusters, $n = 4$–6, are shown in lower panel.

minimum for $n = 6$, and eventually rise again to more than 1 ps for $n = 15$. A complete summary on the VDE shifts and time constants τ_{shift} for all the cluster sizes is given in Table 1.

The increase in VDE is accompanied by a slight broadening of the spectra. For the smaller clusters ($n = 4$–6), the FWHM is 260 meV at time zero, increases by 20–30 meV until ~200 fs, and remains constant at longer pump–probe delays. The larger clusters ($n = 8$, 10, 15) exhibit an initial FWHM of 290–300 meV at time zero and reach their maximum value of 350 meV by 400 fs ($n = 8$) and 1 ps ($n = 10$ and 15). At longer delays, no significant change in the width of the spectra is observed. In addition, as the clusters become larger, the electron intensity peaks at longer delay times. The absolute maximum of the signal is reached by 600, 1250, 1500, 1300, 1800 and 2250 fs for the sizes $n = 4$, 5, 6, 8, 10, and 15, respectively. Ultimately at much longer pump–probe delays, the signal decays with a time constants τ_{decay} of several tens of picoseconds, as summarized in Table 2.

Discussion

In the following section we first discuss the implications of the $I^-(NH_3)_n$ results on possible cluster structures and energetics. In the second part, we compare excited state dynamics in $I^-(NH_3)_n$ and $I^-(H_2O)_n$ clusters.

A. $I^-(NH_3)_n$

As a starting point for interpreting our experiments, it would be very useful to know the ground state structures of the $I^-(NH_3)_n$ clusters studied. Unfortunately, in contrast to $I^-(H_2O)_n$ clusters,

Table 1 Short-time behavior ($\Delta t_{delay} \leqslant 3$ ps) of the $I^-(NH_3)_n$ and $I^-(water)_n$ clusters: VDE shifts (ΔVDE) and associated time constants τ_{shift}

	$I^-(NH_3)_n$		$I^-(D_2O)_n/I^-(H_2O)_n^a$	
n	ΔVDE/meV (±5 meV)	τ_{shift}/fs (±5%)	ΔVDE/meV (±5 meV)	τ_{shift}/fs (±5%)
4	69	780	40/55	420/360
5	97	670	270/230	250/270
6	112	595	265/275	270/300
7			360	935
8	211	700	400	980
9	235	660[b]	360	930[b]
10	220	885	400	1050[b]
12	256	835		
13	248	960		
15	233	1010		

[a] The values for the $I^-(water)_n$ clusters are taken from a time interval starting at 200 fs. Within the interval 0–200 fs, $I^-(D_2O)_4$ and $I^-(H_2O)_4$ show a rapid shift of 70 meV and 40 meV, respectively. For $n = 5$ and 6, no significant shift is observed in this early time interval. [b] Uncertainty: ±30%.

no infrared spectroscopic data are available, nor have any electronic structure calculations been performed. (Recently, infrared spectra of $Cl^-(NH_3)_n$ clusters have been obtained by Okumura and co-workers.[42]) The best one can do at this stage is to infer structural motifs from energetics, using comparisons with previous results on halide · water clusters.

Electronic structure[36,43] and molecular dynamics[44,45] calculations on $I^-(H_2O)_n$ clusters predict that the halide binds to the surface of a hydrogen-bonded network of water molecules. Chemical reactivity experiments by Viggiano and co-workers[46] indicate that this "surface" structure holds out at least to $n = 13$. This general configuration reflects the balance between iodide · water and water · water interactions. Cheshovsky and co-workers[47,48] obtained $E_{stab} = 450$ meV for the stabilization energy of $I^-(H_2O)$ [*i.e.*, VDE($n = 1$) − VDE($n = 0$)] (a more refined value of 389 meV was determined from the ZEKE spectrum of Bassman *et al.*[49]), while for the dimer dissociation energy $D_0[(H_2O)_2]$ a value of 150 meV is found.[50] In contrast, a much stronger halide · water interaction such as that between F^- and H_2O leads to "interior" structures in which the F^- is surrounded by water molecules for clusters as small as $n = 4$.[46,51,52]

Similar energetic arguments can be applied to ammonia. The one-photon photoelectron spectra in Fig. 2 and the energetics plotted in Fig. 3 show that $E_{stab} = 260$ meV for $I^-(NH_3)$, and calcu-

Table 2 Long-time behavior of the $I^-(ammonia)_n$ and $I^-(water)_n$ clusters: time constants τ_{decay} of the decay of the overall signal

	τ_{decay}/ps	
n	$I^-(NH_3)_n$	$I^-(D_2O)_n/I^-(H_2O)_n$
4	12 ± 0.2	2.8 ± 0.2
5	21 ± 0.9	37 ± 1
6	22 ± 0.9	96 ± 3
7		300 ± 10
8	28 ± 3.9	440
9		630
10		490
15	53	

lations based on a recent potential energy surface that reproduces high resolution spectroscopic data for this species yield $D_0[(NH_3)_2] = 79$ meV.[53] Both values are slightly more than half of the corresponding H_2O values. We therefore expect $I^-(NH_3)_n$ clusters to be more similar to $I^-(H_2O)_n$ than $F^-(H_2O)_n$ clusters with surface rather than interior structures likely over the size range probed in our experiment.

We next consider the dynamics seen in our FPE spectra, specifically the increase in VDE with time. Physically, the pump pulse ejects the excess electron from the relatively compact 5p atomic orbital on the iodide into a much more diffuse orbital. While the initial configuration of NH_3 molecules in the ground state of an $I^-(NH_3)_n$ cluster is optimal for solvation of the I^-, the energy shifts in our FPE spectra indicate that this geometry is not the lowest energy configuration for the cluster excited state, and that the solvent molecules rearrange in order to stabilize the excess electron; this is the process referred to henceforth as "partial solvation," in analogy to our previous results on $I^-(water)_n$ clusters.[28] The actual value of the energy released by this process cannot be obtained directly from the spectra, since the increase in VDE reflects the difference between the anion and neutral cluster energies at the anion geometry, not simply the stabilization of the excess electron brought about by solvent rearrangement. Nonetheless, the trend in Table 1 is toward larger shifts with increasing cluster size, and certainly suggests that solvent rearrangement results in more stabilization for the larger clusters.

The spectral shift is irreversible and is accompanied by relatively little broadening. This implies that the energy released by the solvent reorganization flows into the many vibrational modes of the cluster, most of which are expected to be Franck–Condon inactive with respect to photodetachment. Another important aspect of the FPE spectra is the overall *increase* in the intensity of the electron signal during the first picosecond after the pump pulse has terminated (as seen in the contour plots of Fig. 4). This cannot be due to a build-up of population in the upper state, since the pump pulse lasts only $\sim$100 fs. Instead, it must reflect an increase in the photodetachment cross-section caused by the solvent reorganization, indicating that the wavefunction for the excess electron changes significantly during this process.

Our observation of excited states with lifetimes in the picosecond range for clusters with as few as four NH_3 molecules is interesting in light of the experimental and theoretical work on negatively charged, pure $(NH_3)_n^-$ clusters. Haberland and collaborators[16,17] were able to prepare stable ammonia cluster anions *via* capture of low-energy electron in a co-expansion of NH_3 and Ar. However, no evidence was found for stable $(NH_3)_n^-$ with fewer than 35 NH_3 molecules. For comparison, calculations by Jortner and co-workers[18] predict the existence of stable "internal" states of $(NH_3)_n^-$ clusters with positive adiabatic detachment energies (ADEs) for $n \geqslant 32$. This apparent close agreement suggests that the $(NH_3)_n^-$ clusters seen experimentally correspond to internal states, although the calculated VDEs are substantially higher than the experimental values.

On the other hand, calculations by Barnett *et al.*[18] and Marchi *et al.*[19] predict that smaller clusters such as $n = 16$ and 24 only support surface states in which the excess electron is very diffuse and located largely outside the solvent network. For these states, the calculated ADE is either negative or very small, *i.e.*, -0.020 eV for $(NH_3)_{16}^-$, although their VDEs are found to be positive, *i.e.*, 0.21 and 0.34 eV for $(NH_3)_{16}^-$ and $(NH_3)_{24}^-$, respectively.[18] These VDEs are in the range of what we find our "final" solvated states; the long-time VDE for $I^-(NH_3)_{15}$ is 0.42 eV, for example. This comparison thus suggests similarities between the partially solvated excited states in our experiment and the surface states in $(NH_3)_n^-$ clusters.

B. Comparison of $I^-(NH_3)_n$ with $I^-(water)_n$

In order to facilitate comparison between the present results for $I^-(NH_3)_n$ with those for $I^-(H_2O)_n$, Tables 1 and 2 also include values obtained for the water systems; the values for $n \leqslant 6$ have been published previously[28] and those for the larger clusters are preliminary. In addition, the time-dependent VDEs for $I^-(D_2O)_n$ ($n = 4$–6) are shown in the lower panel of Fig. 5; those for $I^-(H_2O)_n$ are similar.

There are clear differences between the FPE spectra of the two cluster families. (1) While the VDEs in $I^-(NH_3)_n$ clusters shift smoothly with time, the VDEs for I^- $(H_2O)_n$ and $I^-(D_2O)_n$ ($n \geqslant 5$) remain relatively constant for 250–500 fs and then rapidly shift to a higher value. (2) The

I^-(ammonia)$_n$ clusters reveal a gradual increase in VDE shift with increasing cluster size, whereas the I^-(water)$_n$ clusters show an abrupt increase in the VDE shift going from $n = 4$ (40 meV) to $n = 5$ (210 meV). In addition, the "final" VDEs after 2–3 ps are significantly larger for I^-(water)$_n$ clusters than for comparably-sized $I^-(NH_3)_n$ clusters. (3) The long-time decay dynamics differ between both solvent species. Except for the $n = 4$ clusters, the time constants of the overall signal decay for $I^-(NH_3)_n$ are significantly shorter than those obtained for I^-(water)$_n$.

We first focus on the different short-time dynamics seen for the two cluster families. The $I^-(H_2O)_4$ FPE spectrum was attributed to excitation to a dipole-bound state (DBS) that decays rapidly by vibrational autodetachment. For $n \geqslant 5$, the relatively constant VDE at early time and the subsequent shift were interpreted as initial excitation to a DBS of the solvent network followed by electron solvation through solvent rearrangement. In the $I^-(NH_3)_n$ spectra, the VDE shifting begins right away, implying that there is no initially excited DBS. The absence of the DBS suggests that the dipole moment of the solvent network is less than the critical value of 2–2.5 D needed to support such a state.[54,55]

This result is not entirely unexpected based on the properties of the bare clusters. While water has a slightly larger dipole moment than NH_3 (1.85 *vs.* 1.47 D), the dipole moment of $(H_2O)_2$ is significantly larger than that of $(NH_3)_2$ (2.65 D *vs.* 0.74 D).[50,56] The smaller dipole in $(NH_3)_2$ originates from much smaller barriers between equivalent minima on the potential energy surface,[53] resulting in large amplitude motion in the vibrational ground state and a lower dipole than would be obtained from a rigid structure. As a result, $(H_2O)_2^-$ has been observed and assigned to be a DBS,[57] whereas $(NH_3)_2^-$ has never been observed. The importance of large amplitude vibrational motion has not been addressed for larger neutral ammonia clusters, ammonia cluster anions or halide·(ammonia)$_n$ clusters. Nonetheless, while several $(H_2O)_n^-$ clusters ($3 \leqslant n \leqslant 11$) have been observed and predicted to be dipole-bound states,[58–62] no $(NH_3)_n^-$ anions in this size range have been identified.

Based on these considerations, one would certainly expect a lesser role for dipole-bound states in $I^-(NH_3)_n$ clusters than in $I^-(H_2O)_n$ clusters. Moreover, our clusters are generally not in their vibrational ground state; we estimate the vibrational temperature to lie between 50–200 K. Infrared spectroscopy experiments by Johnson and co-workers[63] have already hinted that finite vibrational temperatures can weaken or break up the solvent network in halide·$(H_2O)_n$ clusters. Given the weaker interaction between NH_3 molecules compared to H_2O molecules, such effects are likely to be even more important in $I^-(NH_3)_n$ clusters, further diminishing the likelihood of a solvent network with a high dipole moment. This picture is consistent with the preliminary IR spectra by Okumura and co-workers[42] on $Cl^-(NH_3)_n$ clusters.

Fig. 6 shows a schematic picture of the dynamics occurring in both cluster types subsequent to the pump excitation; one-dimensional potential energy curves as a function of solvent coordinate are shown for the ground and excited states. For $I^-(NH_3)_n$ clusters (Fig. 6a), the spectra are consistent with direct access of the excited state surface upon which partial solvation occurs through solvent reorientation; this is represented by a single minimum surface. In contrast, the FPE spectra of the clusters $I^-(H_2O)_n$ and $I^-(D_2O)_n$ ($n \geqslant 5$) suggest that these species are initially photoexcited into a dipole-bound state separated by a barrier from a lower lying conformer in which the electron is more highly solvated (Fig. 6b).

The lower VDEs after 2–3 ps for $I^-(NH_3)_n$ *vs.* $I^-(H_2O)_n$ excited states point to a weaker electron–solvent interaction in the partially-solvated state for the ammonia-containing clusters. This result is consistent with the lower VDEs measured for $(NH_3)_n^-$ *vs.* comparably-sized $(H_2O)_n^-$ clusters, and indeed with the lower threshold for electron ejection from metal–ammonia solutions (1.4 eV) compared to the photoelectric threshold of the hydrated electron (3.2 eV).[17]

A more intriguing result is the much shorter lifetime of the partially-solvated state for $I^-(NH_3)_n$ clusters compared to $I^-(H_2O)_n$ (except $n = 4$); as shown in Table 2, these differ by as much as a factor of 16 for the $n = 8$ clusters. We observe no photofragmentation in our experiments, indicating that decay occurs by electron emission rather than recombination of the electron with the I atom followed by solvent evaporation (to dispose of the resulting 3 eV of energy released if this occurs). *Ab initio* and molecular dynamics calculations on $(H_2O)_n^-$ and $(NH_3)_n^-$ clusters in this size range generally predict positive vertical detachment energies but negative adiabatic detachment energies, so that the cluster anions are metastable with respect to electron detachment.[18,59,60,62,64] Consequently, as the solvent molecules librate and vibrate, they are likely to

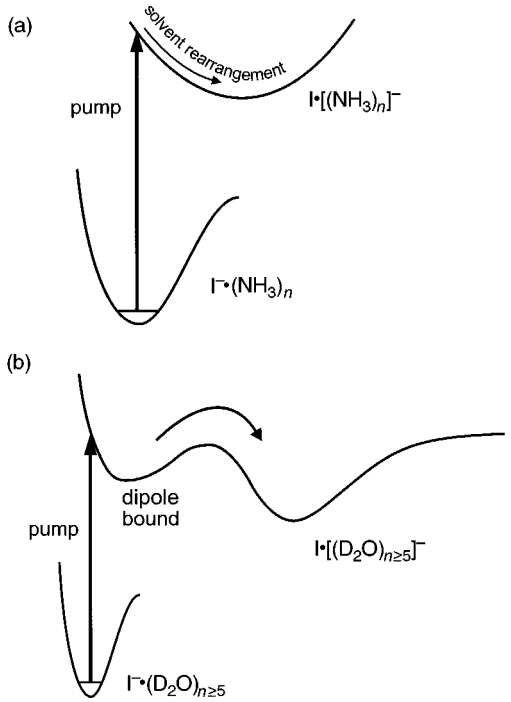

Fig. 6 Schematic display of the dynamics occurring upon excitation of CTTS precursor states in $I^-(NH_3)_n$ (a) and $I^-(D_2O)_{n\geq 5}$ (b), emphasizing the apparent absence of an initially excited dipole-bound state in $I^-(NH_3)_n$ clusters.

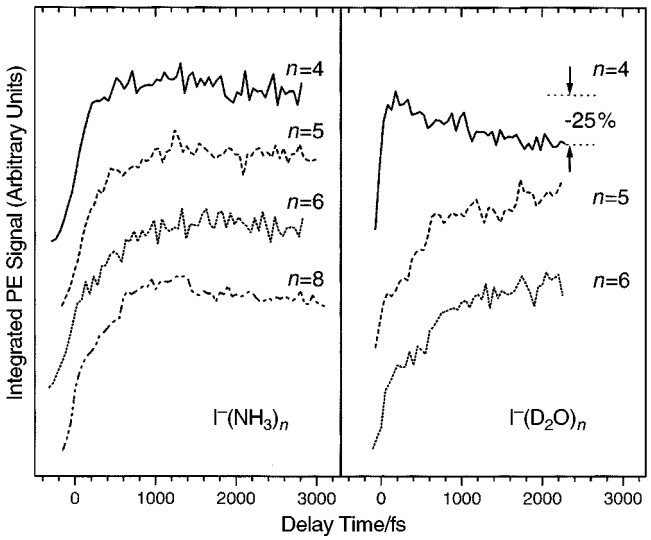

Fig. 7 Integrated photoelectron signal as a function of the delay in the short-time range ($\Delta t_{delay} \leqslant 3$ ps) for $I^-(NH_3)_{n=4-6,8}$ (left) and $I^-(D_2O)_{n=4-6}$ (right). Note that in contrast to all other sizes and solvent species displayed, only $I^-(D_2O)_{n=4}$ shows an immediate onset of signal decay resulting in a 25% decrease by 2.3 ps.

eventually explore configurations for which the electron detachment energy is either very small or negative, at which point electron ejection can occur. One can then rationalize the shorter lifetimes of the $I^-(NH_3)_n$ excited states as another consequence of a flatter potential landscape and larger amplitude motion in ammonia clusters as compared to water clusters, so that the solvent configurations unfavorable to electron binding are sampled more rapidly.

In many aspects, the $n = 4$ water clusters represent an exception among the cluster sizes and molecular solvent species investigated so far (including $I^-(CH_3OH)_n$).[65] Only $I^-(H_2O)_4$ and $I^-(D_2O)_4$ do not show any evidence of electron solvation. They are also the only halide·water clusters for which the lifetime of the excited state is much shorter than that of the comparable $I^-(NH_3)_n$ cluster. The uniqueness of $n = 4$ water clusters is underlined in Fig. 7. Here, the integral PE signal for $I^-(NH_3)_{n=4-8}$ and $I^-(D_2O)_{n=4-6}$ is plotted as a function of the pump–probe delay from 0–3 ps. Only $I^-(D_2O)_{n=4}$ shows any decay on this time scale (decreased by 25% at 2.3 ps) after an exceptionally steep, initial rise. We also note that bare $(H_2O)_4^-$ clusters apparently are very difficult to generate, as evidenced by its absence in all published photoelectron[66,67] and infrared[61] spectroscopy work to date.

Recent calculations by Kim *et al.*[62] show that the most stable form of $(H_2O)_4^-$, a cyclic structure with a high dipole moment, not only is metastable with respect to electron detachment but also is quite similar in geometry to the neutral ground state (also a cyclic structure, but with no dipole moment) and can easily lose its excess electron through internal rotation of two water molecules. The key point here is that Kim *et al.*'s calculated $(H_2O)_4^-$ ground state, in which one O–H bond on each water molecule is directed toward the excess electron, is similar to the structure of the solvent network in the ground state of $I^-(H_2O)_4$.[36] This implies that the DBS formed by excitation of the CTTS band in $I^-(H_2O)_4$ cannot be significantly stabilized by solvent rearrangement, and instead undergoes facile electron ejection, consistent with the apparent absence of solvation dynamics in this cluster.

Conclusions

We have investigated the dynamics of the CTTS states in $I^-(NH_3)_n$ anion clusters, $n = 4$–15, using femtosecond photoelectron spectroscopy. The experiments show that excitation results in a loosely-bound electron that becomes more solvated on a 500 fs–1 ps time scale, and the resulting "partially solvated" state decays by electron emission on a time scale ranging from 10–50 ps. No evidence for an initially excited dipole bound state is seen for $I^-(NH_3)_n$ clusters, in contrast to $I^-(water)_n$ clusters of comparable size. The lifetime of the excited state is generally much shorter in the $I^-(NH_3)_n$ clusters compared to that of the water systems (except $n = 4$). Many of the dynamical features associated with the excited state and the differences between the excited state dynamics in $I^-(NH_3)_n$ and $I^-(water)_n$ clusters can be understood in terms of the properties of neutral and anionic $(NH_3)_n$ and $(H_2O)_n$ clusters.

Future experiments will focus on investigating larger cluster sizes. We are particularly interested in exploring clusters with more than 30 ammonia molecules. This would put us in the size range where interior solvated states are predicted for the bare cluster anions, possibly leading to an abrupt change in the excited state solvation dynamics. It is also of interest to search for photofragmentation of larger clusters subsequent to CTTS excitation. This could be a signature of charge recombination, which is generally believed to be the decay mechanism of solvated electrons in solution.[33–35]

Acknowledgements

This research is supported by the National Science Foundation under Grant No. CHE-9732758. C.F. gratefully acknowledges postdoctoral support from the Leopoldina Akademie with means of the Bundesministerium für Bildung und Forschung, Germany (Grant No. BMBF-LPD 9801-6). A.V.D. is a National Science Foundation pre-doctoral fellow.

References

1 W. Weyl, *Ann. Phys.* (*Leipzig*), 1864, **123**, 350.
2 C. A. Kraus, *J. Am. Chem. Soc.*, 1908, **30**, 1323.

3 J. C. Thompson, *Electrons in Liquid Ammonia*, Oxford University Press, Oxford, 1976.
4 *J. Phys. Chem.*, 1980, **84**, 1065.
5 E. J. Hart and J. W. Boag, *J. Am. Chem. Soc.*, 1962, **84**, 4090.
6 *Adv. Chem. Ser.*, 1965, 50.
7 E. J. Hart and M. Anbar, *The Hydrated Electron*, Wiley-Interscience, New York, 1970.
8 *Electron-Solvent and Anion Solvent Interactions*, ed. L. Kevan and B. C. Webster, Elsevier, New York, 1976.
9 J. H. Baxendale and P. Wardman, *Nature* (*London*), 1971, **230**, 449.
10 J. H. Baxendale and P. Wardman, *J. Chem. Soc., Faraday Trans. 1*, 1973, **69**, 584.
11 A. Migus, Y. Gauduel, J. L. Martin and A. Antonetti, *Phys. Rev. Lett.*, 1987, **58**, 1559.
12 C. Silva, P. K. Walhout, K. Yokoyama and P. Barbara, *Phys. Rev. Lett.*, 1998, **80**, 1086.
13 A. Kummrov, M. F. Emde, A. Baltuska, M. S. Pshenichnikov and D. A. Wiersma, *J. Phys. Chem. A*, 1998, **102**, 4171.
14 X. Shi, F. H. Long, H. Lu and K. B. Eisenthal, *J. Phys. Chem.*, 1995, **99**, 6917.
15 P. K. Walhout, J. C. Alfano, Y. Kimura, C. Silva and P. F. Barbara, *Chem. Phys. Lett.*, 1995, **232**, 135.
16 H. Haberland, H.-G Schindler and D. R. Worsnop, *Ber. Bunsen-Ges. Phys. Chem.*, 1984, **88**, 270.
17 G. H. Lee, S. T. Arnold, J. G. Eaton, H. W. Sarkas, K. H. Bowen, C. Ludewigt and H. Harberland, *Z. Phys. D*, 1991, **20**, 9.
18 R. N. Barnett, U. Landman, C. L. Cleveland, N. R. Kestner and J. Jortner, *Chem. Phys. Lett.*, 1988, **148**, 249.
19 M. Marchi, M. Spirik and M. L. Klein, *J. Chem. Phys.*, 1988, **89**, 4918.
20 L. V. Hertel, C. Hüglin, C. Nitsch and C. P. Schulz, *Phys. Rev. Lett.*, 1991, **67**, 1767.
21 C. Nitsch, C. P. Schulz, A. Gerber, W. Zimmermann-Edling and I. V. Hertel, *Z. Phys. D*, 1992, **22**, 651.
22 P. Brockhaus, I. V. Hertel and C. P. Schulz, *J. Chem. Phys.*, 1999, **110**, 393.
23 F. Misaizu, K. Tsukamoto, M. Sanekata and K. Fuke, *Chem. Phys. Lett.*, 1992, **188**, 241.
24 R. Takasu, K. Hashimoto and K. Fuke, *Chem. Phys. Lett.*, 1996, **258**, 94.
25 R. Takasu, F. Misaizu, K. Hashimoto and K. Fuke, *J. Phys. Chem. A*, 1997, **101**, 3078.
26 K. Hashimoto and K. Morokuma, *J. Am. Chem. Soc.*, 1995, **117**, 4151.
27 D. Serxner, C. E. H. Dessent and M. A. Johnson, *J. Chem. Phys.*, 1996, **105**, 7231.
28 L. Lehr, M. T. Zanni, C. Frischkorn, R. Weinkauf and D. M. Neumark, *Science*, 1999, **284**, 635.
29 J. Franck and G. Scheibe, *Z. Phys. Chem. A*, 1928, **139**, 22.
30 M. J. Blandamer and M. F. Fox, *Chem. Rev.*, 1970, **70**, 59.
31 J. Jortner, M. Ottolenghi and G. Stein, *J. Phys. Chem.*, 1964, **68**, 247.
32 F. H. Long, X. L. Shi, H. Lu and K. B. Eisenthal, *J. Phys. Chem.*, 1994, **98**, 7252.
33 J. A. Kloepfer, V. H. Vilchiz, V. A. Lenchenkov and S. E. Bradforth, *Chem. Phys. Lett.*, 1998, **298**, 120.
34 W.-S Sheu and P. J Rossky, *Chem. Phys. Lett.*, 1993, **202**, 186.
35 A. Staib and D. Borgis, *J. Chem. Phys.*, 1996, **104**, 9027.
36 J. E. Combariza, N. R. Ketner and J. Jortner, *J. Chem. Phys.*, 1994, **100**, 2851.
37 B. J. Greenblatt, M. T. Zanni and D. M. Neumark, *Discuss. Faraday Soc.*, 1997, **108**, 101.
38 B. J. Greenblatt, M. T. Zanni and D. M. Neumark, *Chem. Phys. Lett.*, 1996, **258**, 523.
39 W. C. Wiley and I. H. McLaren, *Rev. Sci. Instrum.*, 1995, **26**, 1150.
40 O. Cheshnovsky, S. H. Yang, C. L. Pettiette, M. J. Craycraft and R. E. Smalley, *Rev. Sci. Instrum.*, 1987, **58**, 2131.
41 M. D. Davidson, B. Broers, H. G. Muller and H. B. van Linden van den Heuvell, *J. Phys. B*, 1992, **25**, 3093.
42 K. T. Kuwata, J. D. Lobo and M. Okumura, unpublished work.
43 J. E. Combariza, N. R. Kestner and J. Jortner, *Chem. Phys. Lett.*, 1994, **221**, 156.
44 L. X. Dang and B. C. Garrett, *J. Chem. Phys.*, 1993, **99**, 2972.
45 L. X. Dang, *J. Chem. Phys.*, 1999, **110**, 1526.
46 A. A. Viggiano, S. T. Arnold and R. A. Morris, *Int. Rev. Phys. Chem.*, 1998, **17**, 147.
47 G. Markovich, R. Giniger, M. Levin and O. Cheshnovsky, *J. Chem. Phys.*, 1991, **95**, 9416.
48 G. Markovich, S. Pollack, R. Giniger and O. Cheshnovsky, *J. Chem. Phys.*, 1994, **101**, 9344.
49 C. Bassmann, U. Boesl, D. Yang, G. Drechsler and E. W. Schlag, *Int. J. Mass Spectrom. Ion Processes*, 1996, **159**, 153.
50 R. S. Fellers, C. Leforestier, L. B. Braly, M. G. Brown and R. J. Saykally, *Science*, 1999, **284**, 945.
51 O. M. Cabarcos, C. J. Weinheimer, J. M. Lisy and S. S. Xantheas, *J. Chem. Phys.*, 1999, **110**, 5.
52 P. Weis, P. R. Kemper, M. T. Bowers and S. S. Xantheas, *J. Am. Chem. Soc.*, 1999, **121**, 3531.
53 E. H. T. Olthof, A. van der Avoird and P. E. S. Wormer, *J. Chem. Phys.*, 1994, **101**, 8430.
54 O. H. Crawford, *Mol. Phys.*, 1971, **20**, 585.
55 C. Desfransois, H. Abdoul-Carime and J. P. Schermann, *Int. J. Mod. Phys. B*, 1996, **10**, 1339.
56 G. T. Fraser, D. D. Nelson, A. Charo and W. Klemperer, *J. Chem. Phys.*, 1985, **82**, 2335.
57 J. H. Hendricks, H. L. de Clercq, S. A. Lyapustina, C. A. Fancher, T. P. Lippa, J. M. Collins, S. T. Arnold, G. H. Lee and K. H. Bowen, in *Structures and Dynamics of Clusters*, ed. T. Kondow, K. Kaya and A. Terasaki, Universal Academy Press, Tokyo, 1996, p. 321.
58 D. M. A. Smith, J. Smets, Y. Elkadi and L. Adamowicz, *J. Chem. Phys.*, 1997, **107**, 5788.

59 D. M. A. Smith, J. Smets, Y. Elkadi and L. Adamowicz, *J. Chem. Phys.*, 1998, **109**, 1238.
60 D. M. A. Smith, J. Smets and L. Adamowicz, *J. Chem. Phys.*, 1999, **110**, 3804.
61 P. Ayotte, G. H. Weddle, C. G. Bailey, M. A. Johnson, F. Vila and K. D. Jordan, *J. Chem. Phys.*, 1999, **110**, 6268.
62 J. Kim, S. B. Suh and K. S. Kim., *J. Chem. Phys.*, 1999, **111**, 10077.
63 P. Ayotte, G. H. Weddle and M. A. Johnson, *J. Chem. Phys.*, 1999, **110**, 7129.
64 S. Lee, J. Kim, S. J. Lee and K. S. Kim, *Phys. Rev. Lett.*, 1997, **79**, 2038.
65 A. V. Davis, M. T. Zanni, C. Frischkorn and D. M. Neumark, *J. Electron Spectrosc Relat. Phenom.*, in press.
66 J. V. Coe, G. H. Lee, J. G. Eaton, S. T. Arnold, H. W. Sarkas, K. H. Bowen, C. Ludewigt, H. Haberland and D. R. Worsnop, *J. Chem. Phys.*, 1990, **92**, 3980.
67 J. Kim, I. Becker, O. Cheshnovsky and M. A. Johnson, *Chem. Phys. Lett.*, 1998, **297**, 90.